

**Effect of High Temperature Corrosion on Austenitic
Stainless Steel Grade 304 in CO₂ Gas at 700°C**
(Kesan Kakisan Suhu Tinggi Terhadap Keluli Tahan Karat Austenit Gred 304
Dalam Persekitaran Gas CO₂ Pada Suhu 700°C)

NURUL ATIKAH SHARIFF, AZMAN JALAR, MUHAMAD IZHAR SAHRI, NORINSAN KAMIL OTHMAN*

ABSTRACT

Austenitic stainless steels of grade 304 were exposed to dry (Ar-75%CO₂) and wet (Ar-75%CO₂-12%H₂O) environments at 700°C. This experimental setup involved horizontal tube furnace connected to CO₂ gas and water vapour facilities. X-ray diffraction (XRD) technique, variable pressure-scanning electron microscope (VP-SEM) and optical microscope techniques were used to characterize the products of corrosion. The results of XRD showed that the phase of oxide layers consists of Cr₂O₃ and NiCr₂O₄ in dry CO₂, meanwhile Fe₂O₃, Cr₂O₃, Fe_{0.56}Ni_{0.34}, Fe₃O₄ were identified in wet condition after 50 h. Adding 12%H₂O in Ar-75%CO₂ leads significantly in weight change occurred at 10 h exposure. However, after 20 h, the weight gain was decreased due to spallation of the oxide scale. The addition of water vapour accelerates the oxidation rate on the steel than that in dry condition. Morphologies and growth kinetics of these oxides vary with reaction condition. The oxidation behaviour at different times of exposure and the effect of water vapour were discussed in correlation with the microstructure of the oxides.

Keywords: Austenitic stainless steel; oxidation; water vapour

ABSTRAK

Keluli tahan karat Austenit gred 304 telah didedahkan dalam persekitaran kering (Ar-75%CO₂) dan basah (Ar-75%CO₂-12%H₂O) pada suhu 700°C. Kajian ini telah menggunakan relau melintang yang dilengkapi dengan aliran gas CO₂ dan kemudahan penghasilan wap air. Teknik pembelauan sinar-X (XRD), mikroskop elektron imbasan pelbagai tekanan (VP-SEM) dan mikroskop optik (OM) telah digunakan untuk pencirian hasil produk kakisan. Hasil keputusan XRD menunjukkan fasa lapisan oksida Cr₂O₃ dan NiCr₂O₄ terbentuk dalam persekitaran kering CO₂, sementara itu Fe₂O₃, Cr₂O₃, Fe_{0.56}Ni_{0.34}, Fe₃O₄ telah dikenal pasti dalam persekitaran basah selepas 50 jam pendedahan. Penambahan 12%H₂O dalam Ar-75%CO₂ membawa kepada perubahan berat yang ketara pada pendedahan selama 10 jam. Walau bagaimanapun, selepas 20 jam, pertambahan berat menurun disebabkan oleh pengelupasan lapisan oksida. Kehadiran wap air mempercepat kadar pengoksidaan terhadap keluli berbanding dalam keadaan kering. Morfologi dan pertumbuhan kinetik lapisan oksida adalah berbeza mengikut keadaan tindak balas. Perilaku pengoksidaan pada masa pendedahan yang berbeza dan kesan wap air telah dibincangkan dengan menghubungkan mikrostruktur oksida.

Kata kunci: Keluli tahan karat Austenit; pengoksidaan; wap air

INTRODUCTION

Austenitic stainless steels are among the best common and familiar types of stainless steels. They are known as nonmagnetic; tremendously formable and weldable and can be successfully used from cryogenic temperatures to the red-hot temperatures of furnaces and jet engines (TMI Society 2008). Austenitic stainless steel grade 304 is extensive and widely used in petrochemical, thermal power plants, boiler part and pressure vessel in a temperature range between 600°C and 850°C, due to the fact of their corrosion resistance at ordinary temperature conditions, costs and mechanical properties. Consequently, applications of austenitic steels are restricted to higher temperature applications and specific situations where severe corrosion conditions occurred (Ishak et al. 2008). Nevertheless, at high temperature with oxidizing or

hazardous atmosphere, the surface of this alloy can be attacked and resulting in the formation of protective to non-protective scales (Young & Watson 1995).

High temperature oxidation performance of alloys in the mixed gas environment has been one of the main scientific and engineering interests in the large field of environmentally induced degradation of materials over the past 18 years (Rouillard et al. 2009). It is well known that parts of boiler system are exposed to high temperature oxidation and hot corrosion that are recognized as the main factors for degradation of boiler parts. In general, most of the metals are thermodynamically unstable with respect to ambient gases such as CO, O₂ and CO₂ at elevated temperature. Finally, the gas reacts with the surface of boiler part to form different compounds such as oxide or spinel. The certain compounds may protect the underlying

metals or may also thicken into a non-protective scale with various defects such as cavities, microcracks and porosities as shown in Figure 1 (Rujisomnana et al. 2010).

Many service environments contain combustion products, such as water vapour and carbon dioxide compounds. All have a harmful influence on oxidation resistance of the underlying metals. Furthermore, it is well recognized that oxide films are ductile at high temperature and are often brittle at lower temperature. Most oxide films have different thermal expansion coefficients with those of the underlying metals from which they are formed. Therefore, the oxide films formed at a high service temperature may lose adherence to the underlying metals, when cooled to lower temperature and turn into the non-protective films. These are the major reasons for breakaway oxidation and degradation of the underlying metals (Othman et al. 2010).

In the process of oxyfuel combustion, the oxygen is required to separate from air prior combustion and the fuel is combusted in oxygen diluted with recycled flue-gas rather than by air. The oxygen-rich, nitrogen-free atmosphere results in final flue-gases consisting mainly of CO_2 and H_2O (water). Specific concern for corrosion is the presence of water vapour in the exhaust gas as a combustion product. The presence of water vapour is identified to increase the corrosive tendency of the environment. Water vapour can affect this process in the various ways. It has been well-known that the presence of water vapour in oxidizing environments can accelerate the degradation process for many different metals including austenitic stainless steel (Kumar et al. 2011).

In order to understand the effect of the water vapour on high temperature oxidation behavior, austenitic stainless steel grade 304 was selected to be studied in CO_2 gas with the presence of water vapour content. Additional of 12% H_2O in 75% CO_2 gas was used to stimulate the gases that mainly found in fossil fuel combustion.

MATERIAL AND EXPERIMENTAL METHODS

The austenitic stainless steel grade 304 model alloys were used to investigate the effect of dry gas and also in addition with water vapour. The chemical compositions of austenitic stainless steel grade 304 were shown in Table 1. Ten sample coupons were cut into square shapes about $10 \times 10 \times 2 \text{ mm}^3$, ground to 1200 grit finish and ultrasonically cleaned in ethanol immediately prior exposure. The alloy coupons were subjected to an isothermal condition to the horizontal tube furnace (Figure 2) in flowing Ar-75% CO_2 and Ar-75% CO_2 -12% H_2O atmospheres with a flow rate of 200 mL/min at 700°C for different reaction time exposure (10, 20, 30, 40 and 50 h). The 12% water vapour was produced when the gas flowed through a water bath condenser system at 50°C (Mikkelsen & Linderoth 2003). The isothermal experiment was performed by moving the sample into the hot zone. Samples were weighted initially and reweighed, for each reaction time. The weight gain was calculated by measuring the weight difference. The oxidized coupons were analysed using X-ray diffraction (XRD) to identify the reaction products. The scale morphologies were characterized using optical metallography and variable pressure-scanning electron microscope.

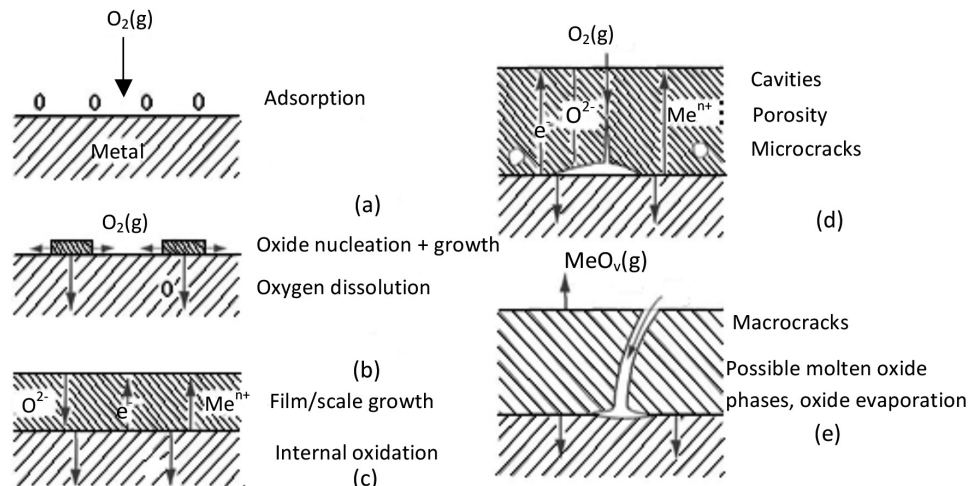


FIGURE 1. Film and scale formations during high-temperature oxidation

TABLE 1. Chemical composition of the austenitic stainless steel grade 304 in wt.%

Element	C	Mn	Si	P	S	Cr	Ni	Fe
wt.%	0.08	2.00	1.00	0.04	0.04	20.00	10.00	Balance

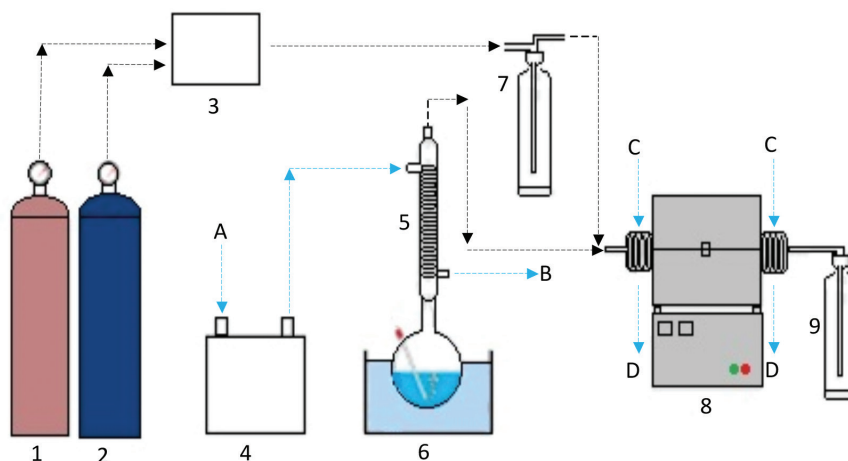


FIGURE 2. Experimental setup for high temperature apparatus; (1) carbon dioxide gas, (2) argon gas, (3) flow meter, (4) water tank, (5) condenser, (6) water bath, (7) drying tower, (8) horizontal tube furnace, (9) gas trap (A) water inlet, (B) water outlet, (C) coolant inlet and (D) coolant outlet

RESULTS AND DISCUSSION

The weight change measurement of austenitic stainless steel grade 304 as a function of time at 700°C in dry CO₂ and in the presence of water vapour are shown in Figure 3. In dry gas, very low weight gain of up to 0.001 g was observed for the sample oxidized after 50 h exposure. However, significant weight gain was observed at 10 h exposure in wet condition and very low weight gain was up to 50 h. Scale composition was investigated by using X-ray diffraction and represented in Table 2. From the XRD

analysis, chromium oxide (Cr₂O₃) and nickel chromium oxide (NiCr₂O₄) were found in dry CO₂ whereas phases of Cr₂O₃, FeO, Fe₃O₄, Fe₂O₃ and Fe_{0.56}Ni_{0.34} were displayed in wet condition. The addition of water vapour significantly change the weight gain at 700°C.

Figure 4 shows the photographs of scale surfaces produced in the austenitic stainless steel after different time exposure. Fine grained and dark oxides were observed in dry CO₂. Nonetheless, in wet condition, many cracks and spallation were clearly found on the surface after reaction.

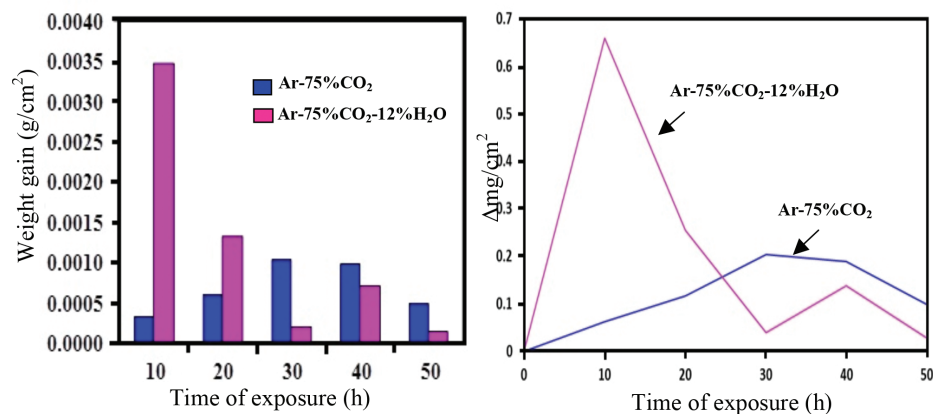


FIGURE 3. Weight change measurements in Ar-75%CO₂ and Ar-75%CO₂-12%H₂O

TABLE 2. Surface reaction product identified by XRD after 50 h exposure in Ar-75%CO₂ and Ar-75%CO₂-12%H₂O

Exposure times (h)	Dry (Ar-75%CO ₂)	Wet (Ar-75%CO ₂ -12%H ₂ O)
10	Cr ₂ O ₃ , NiCr ₂ O ₄	Cr ₂ O ₃ , FeO, FeCr ₂ O ₄ , Fe _{0.54} Ni _{0.36}
30	Cr ₂ O ₃ , NiCr ₂ O ₄	Cr ₂ O ₃ , Fe _{0.56} Ni _{0.34} , Fe ₃ O ₄
50	Cr ₂ O ₃ , NiCr ₂ O ₄	Cr ₂ O ₃ , Fe _{0.56} Ni _{0.34} , Fe ₂ O ₃ , Fe ₃ O ₄

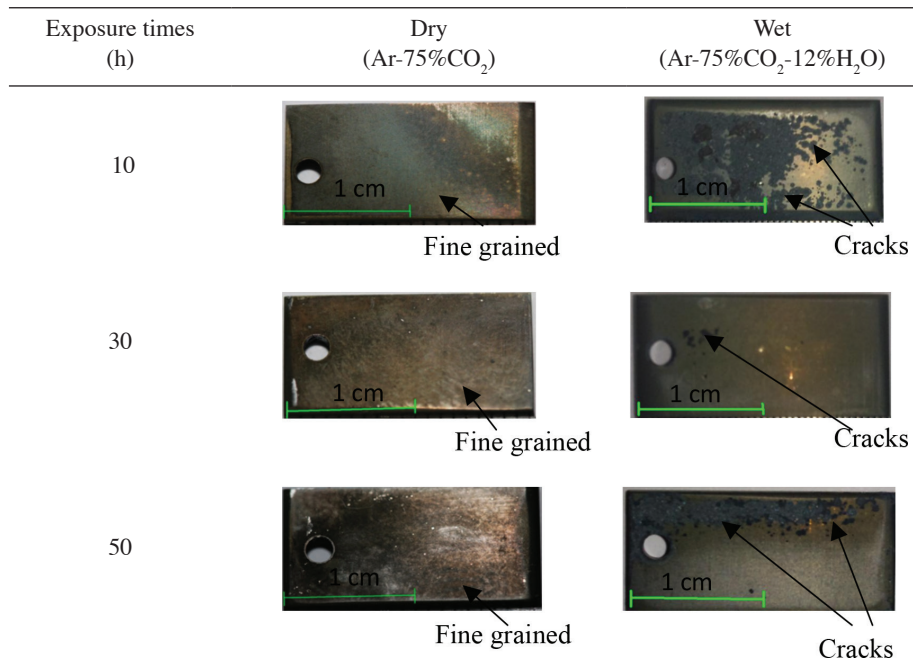


FIGURE 4. Camera ready images of sample after exposure in dry and wet conditions

No whiskers were exhibited in both dry and wet conditions (Figure 5). Most of the oxide whiskers were long, very thin and have a uniform thickness tunnel along the axis of the needles and platelets, allowing fast surface diffusion of cations along the tunnel (Polman et al. 1989).

A cross section of the austenitic stainless steel interface analysed using optical microscope, is shown in Figure 6. Polished cross-section in dry CO₂ gas showed a thin layer after 10 to 50 h of exposure. Meanwhile, the oxide scales

became thicker after 50 h exposure in the presence of water vapour. The metal oxide and substrate region can be clearly seen in Figures 6 and 7.

From the previous study by Chia and Wen (2009), in the reducing gas atmosphere, oxidation besides carburization can occur, resulting in the formation of oxide below carbon deposit. The combined carburization and oxidation processes in a reducing gas atmosphere have been addressed by Grabke (1998), Szakalos et al. (2002),

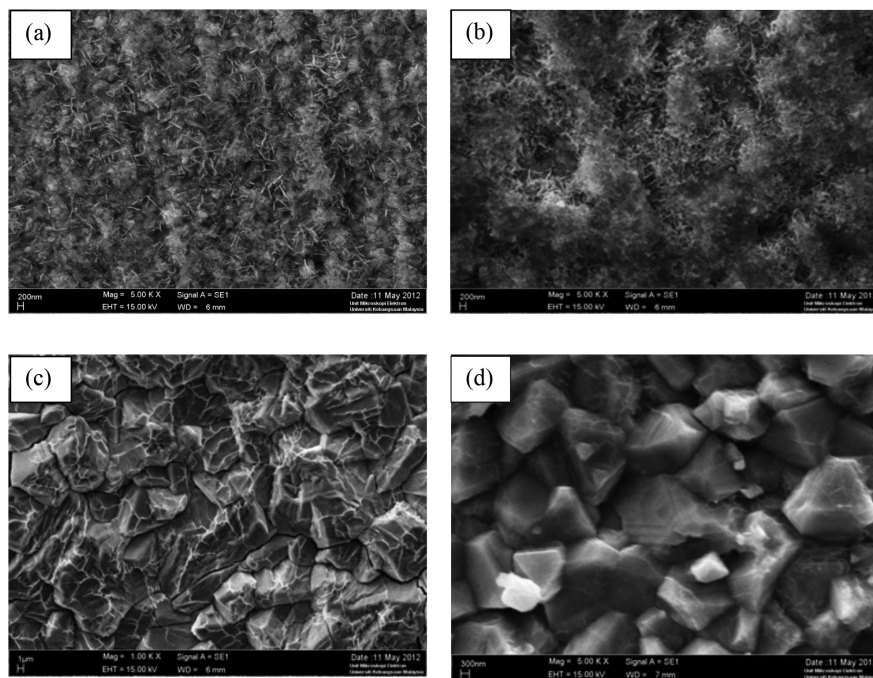


FIGURE 5. SEM micrographs of sample after exposure; a) 10 h in dry CO₂, b) 10 h in wet CO₂, c) 50 h in dry CO₂ and d) 50 h in wet CO₂

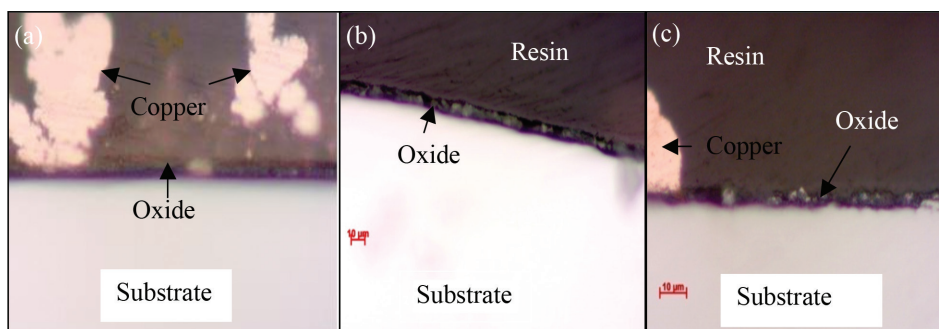


FIGURE 6. Cross section of sample after exposure in dry CO_2 after; a) 10 h, b) 30 h and c) 50 h

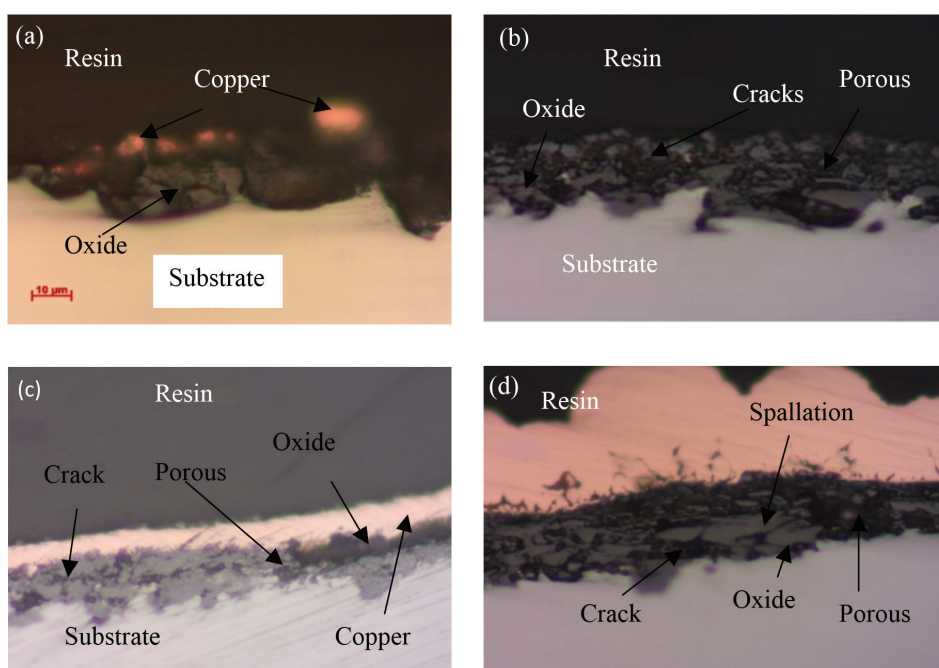
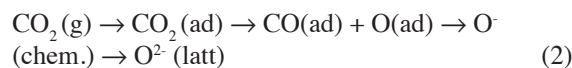
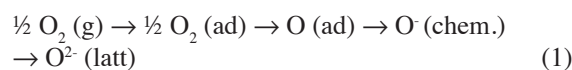


FIGURE 7. Cross section of sample after exposure in wet CO_2 ; a) 10 h, b) 30 h, c) 40 h and d) 50 h with 100 \times magnification

Wuchina et al. (2009) and Young (2008). The presence of the Cr-depleted zone below the external oxide was due to selective or preferential oxidation of Cr, which is common for stainless steel. Chia and Wen (2009) found that when extending the exposure time for a longer period, the oxidation and carburization processes continued to proceed in the $\text{CO}/\text{H}_2/\text{H}_2\text{O}$ mixed gas environment. These processes lead to the successive formation of a Cr-depleted substrate containing voids and the underlying carburized layers.

In the presence of CO_2 in 700°C , oxidation takes place instead of carburization due to dissociation of CO_2 . The processes can be split into several steps at the scale interface. The reactant - gas molecule must move towards the surface and become adsorbed there. The adsorbed molecules then split to form adsorbed oxygen, which finally attracts electrons from the oxide lattice to become initially chemisorbed and eventually integrated into the lattice (Freund & Robert 1996). These processes can be expressed as follows:



From (2), CO_2 adsorbs onto the oxide surface and there dissociates to adsorb CO and O species. In fact, the adsorbed oxygen then goes through the ionization stages. Oxygen turns into dominant and react with the substrate (Liu et al. 2012). The oxide phases found were Wustite (FeO), Magnetite (Fe_3O_4) and Hematite (Fe_2O_3) in iron after exposure to CO_2 gas (Huenert et al. 2008). It can be explained by following reactions:





In dry (Ar-75%CO₂) environments, protective oxide scale which is Cr₂O₃ layer was developed. The capability of the austenitic stainless steel to form protective oxide scale is based on Cr content (Francis 1966). The oxide scale of austenitic stainless steel was found to be adhesive and dense in dry CO₂ especially between metal-oxide interfaces, as seen in Figure 6. From the cross sectional observation, it can be seen that diffusion of oxygen through scale was less in dry CO₂ which showed that the corrosion attack was slower in dry condition.

The aim of this characterization was to obtain a better understanding of the effect of water vapour in flowing CO₂ gas on samples as well. The presence of water vapour in the CO₂ environment accelerated the oxidation of austenitic stainless steel alloys. This indicates that non-protective scale growth occurs in the Ar-75%CO₂-12%H₂O. The presence of water vapour causes acceleration of the oxide growth from protective oxide to non-protective oxide scale. It leads to a significant increase in oxidation rates and thickening the oxide scale due to the formation of non-protecting Fe₃O₄ oxides.

Water vapour significantly affects the performance of this alloy at 700°C. From the cross sectional observation (Figure 7), oxide interface has many voids and become more porous. It was clear that water vapour can accelerate the corrosion rate through the voids or gaps and as a result of low adhesive scale. Metallography of the specimens showed a slightly rough metal-scale interface with the addition of water vapour (Kofstad 1988). Due to crack and porous in wet CO₂ condition, the oxygen penetrates into the substrate and in turn oxidation rate was higher.

In addition, oxidation lead to the cracking of the scale due to the mismatch in coefficient of thermal expansion in oxide scales. As there were various elements and each had different thermal coefficient of expansion hence there will be more stress generated which leads to more cracking (Fujii & Meussner 1964). This effect can be explained as follows. Through this cracks, corrosive gases can penetrate to the base material to accelerate the corrosion attack. Also water vapour has been shown to encourage a more porous scale to form, which was linked to increased cation diffusion, resulting in vacancy condensation forming the pores. Water vapor affects the oxide growth at all stages of the oxidation process such as adsorption, dissociation and diffusion. The pores in the oxide structure assist the rapid inward diffusion of oxygen to form oxide at the metal interface and the pores gradually move outwards to the scale gas interface (Ikeda & Nii 1984).

CONCLUSION

The high temperature oxidation behaviour of austenitic stainless steel was studied in Ar-CO₂ and Ar-CO₂-H₂O at 700°C. This oxidation behavior can be concluded as an oxidation process takes place instead of carburization

due to dissociation of CO₂ become adsorb CO and O species lead to oxygen become dominant and react with the substrate. In dry CO₂, the protective oxide layer was observed to withstand deteriorate steel at high temperature corrosion. Furthermore, the presence of water vapour in CO₂ gas found to be thickened of oxide scale than that in dry CO₂. Oxide scale of austenitic stainless steel grade 304 become porous in the presence of water vapour. However, in dry condition, the oxide scale found to be dense and the protective layer (Cr₂O₃) was still remained. Nevertheless, in wet condition, the protective layer turns into non-protective (Fe₃O₄ and Fe₂O₃) layer after 50 h exposure.

ACKNOWLEDGMENTS

This study was financially supported by UKM GGPM-NBT-089-2010, FRGS/1/2011/ST/UKM/02/14, ERGS/1/2012/ST 205 UKM/02/2, Zamalah Research University Scholarship, DIP 2012-2014 and University and Centre for Research and Instrumentation Management (CRIM), UKM.

REFERENCES

- Chia, H.C. & Wen, T.T. 2009. Carburization behavior under the pits induced by metal dusting in 304L and 347 stainless steels. *Materials Chemistry and Physics* 116: 426-432.
- Francis, J.M. 1966. Influence of minor alloying elements on structure of surface oxides formed during high-temperature oxidation of austenitic steel. *Journal of the Iron and Steel Institute* 204: 910.
- Freund, H.J. & Robert, M.W. 1996. Surface chemistry of carbon dioxide. *Surface Science Reports* 25: 225-273.
- Fujii, C.T. & Meussner, R.A. 1964. The mechanism of the high temperature oxidation of iron-chromium alloys in water vapour. *Journal of the Electrochemical Society* 111(11): 1215-1221.
- Grabke, H.J. 1998. *Carburization: A high temperature corrosion phenomenon*. USA: Materials Technology Institute of the Chemical Process Industries.
- Huenert, D., Schulz, W. & Kranzmann, A. 2008. Corrosion of steels in H₂O-CO₂ atmospheres at temperatures between 500°C and 700°C. Berlin, Germany: Federal Institute of Materials Research and Testing.
- Ikeda, Y. & Nii, K. 1984. Mechanism of accelerated oxidation of Fe-Cr alloys in water vapour containing atmosphere. *Transaction of National Research Institute of Metals* 26(1): 52-62.
- Ishak, H.M., Amin, M.M. & Derman, M.N. 2008. Effect of temperature on corrosion behaviour of AISI 304 stainless steel with magnesium carbonate deposit. *Journal of Physical Science* 19(2): 137-141.
- Kofstad, P. 1988. *High Temperature Corrosion*. London: Elsevier Applied Science.
- Kumar, V., Arora, N. & Singh, S. 2011. Effect of cyclic oxidation behaviour of German steel and austenitic stainless steel. *MIT International Journal of Mechanical Engineering* 1(2): 79-83.
- Liu, L., Zhao, C. & Li, Y. 2012. Spontaneous dissociation of CO₂ to CO on defective surface of Cu(I)/TiO₂ nanoparticles at room temperature. *The Journal of Physical Chemistry* 116(14): 7904-7912.

- Mikkelsen, L. & Linderoth, S. 2003. High temperature oxidation of Fe-Cr alloy in O₂-H₂-H₂O atmospheres: Microstructure and kinetics. *Material Science Engineering A* 361(10): 198-212.
- Othman, N.K., Othman, N. & Zhang, J. 2010. Water vapour effect of cyclic oxidation on Fe-Cr alloys. *Sains Malaysiana* 39(2): 249-259.
- Polman, E.A., Fransen, T. & Gellings, P.J. 1989. Oxidation kinetics of chromium and morphological phenomena. *Oxidation of Metals* 32: 1989.
- Rouillard, F., Cabet, C., Wolski, K. & Pijolat, M. 2009. Oxidation of a chromia-forming nickel base alloy at high temperature in mixed diluted CO/H₂O atmospheres. *Corrosion Science* 51(4): 752-760.
- Rujisomnana, Patharaporn Seechompoo, Porntip Suwannachaoat, Sanganwong Suebca & Pornwasa Wongpanya. 2010. High temperature oxidation behaviour of low carbon steel and austenitic stainless steel. *Journal of Metals, Materials and Minerals* 20(3): 31-36.
- Szakalos, P., Pettersson, R. & Hertzman, S. 2002. An active corrosion mechanism for metal dusting on 304L stainless steel. *Corrosion Science* 44: 2253-2270.
- TMI Society. 2008. *Austenitic Stainless Steels*. Ohio, USA: ASM International.
- Wuchina, E., Opila, E., Fergus, J., Maruyama, T. & Shifler, D. 2009. *High Temperature Corrosion and Materials Chemistry*. Pennington, USA: The Electrochemistry Society.
- Young, D.J. & Watson, S. 1995. High-temperature corrosion in mixed gas environments. *Oxidation of Metals* 44(1-2): 163-190.
- Young, D. 2008. *High Temperature Oxidation and Corrosion of Metals*. Amsterdam, Netherlands: Elsevier.

School of Applied Physics
Faculty of Science and Technology
Universiti Kebangsaan Malaysia
43600 Bangi, Selangor
Malaysia

*Corresponding author; email: insan@ukm.edu.my

Received: 27 March 2013

Accepted: 24 February 2014